

Quark mean field model with pion and gluon corrections

Xueyong Xing, Jinniu Hu,^{*} and Hong Shen

School of Physics, Nankai University, Tianjin 300071, China

(Received 30 June 2016; revised manuscript received 8 August 2016; published 10 October 2016)

The properties of nuclear matter and finite nuclei are studied within the quark mean field (QMF) model by taking the effects of pions and gluons into account at the quark level. The nucleon is described as the combination of three constituent quarks confined by a harmonic oscillator potential. To satisfy the spirit of QCD theory, the contributions of pions and gluons on the nucleon structure are treated in second-order perturbation theory. In a nuclear many-body system, nucleons interact with each other by exchanging mesons between quarks. With different constituent quark mass, m_q , we determine three parameter sets for the coupling constants between mesons and quarks, named QMF-NK1, QMF-NK2, and QMF-NK3, by fitting the ground-state properties of several closed-shell nuclei. It is found that all of the three parameter sets can give a satisfactory description of properties of nuclear matter and finite nuclei, moreover they also predict a larger neutron star mass around $2.3M_{\odot}$ without hyperon degrees of freedom.

DOI: [10.1103/PhysRevC.94.044308](https://doi.org/10.1103/PhysRevC.94.044308)

I. INTRODUCTION

The nucleon, as an element of nuclear physics, is composed of more microscopic particles, named quarks in the standard model. Quarks are confined in the nucleon and interact with each other by exchanging gluons in the basic theory of strong interaction, quantum chromodynamics (QCD). Such confinement will increase hugely with the distance between two quarks. Therefore, it is impossible to observe free quarks in the universe except at some extreme conditions such as high density and high temperature.

At a nuclear energy level, the interaction between quarks cannot be treated with perturbation theory, whose coupling strength is not small anymore. Until now, we still could not describe the nucleon structure as a few-body problem based on the degrees of freedom of quarks and gluons directly with QCD theory as in *ab initio* calculation. With the development of computer technology, the mass spectrum of baryons and mesons has been calculated with lattice QCD theory as a few-quarks system, which can treat the quark confinement very well with numerical methods. The mass spectrum of mesons and baryons was reproduced very well compared to experiment observations [1].

However, it is a big challenge to study a nuclear many-body system based on the degrees of freedom of quarks and gluons with QCD theory, which will help us understand nuclear physics more fundamentally. To overcome such a difficult problem, a lot of many-body methods were proposed, which can reasonably give the properties of finite nuclei from the light mass region to very heavy mass region very well, such as the Green's function Monte Carlo (GFMC) method [2], the shell model [3], Skyrme Hartree-Fock (SHF) theory [4], relativistic mean field (RMF) theory [5], and so on. However, in most of these models, the nucleon is usually treated as a point particle, which does not consider its internal structure. This assumption is against the observation of present experiments about the

nucleon structure. Furthermore, the medium modification of the nucleon structure function [the EMC (European Muon Collaboration) effect] cannot be achieved by treating the nucleon as a point particle. It is a challenge to develop a model for understanding the change of the nucleon structure in nuclei from quark degrees of freedom.

Therefore, Guichon proposed an exploratory model to study the nuclear many-body problem, where the quarks are confined in a bag, as in the MIT bag model, and interact with each other at different nucleons through exchange of σ and ω mesons [6]. The mechanism of nuclear saturation properties can be discussed in terms of quark degrees of freedom. Later, Saito and Thomas *et al.* extended such a model to include more mesons, such as the ρ meson, called the quark-meson coupling (QMC) model [7–9]. The QMC model can be regarded as an extension of the RMF model, where the scalar coupling constant, generated from the effective nucleon mass, is changed with the quark mass in the nuclear medium. Actually, it corresponds to the nuclear EMC effect [10], which modifies the nucleon structure in the nuclear medium. The persistently developed QMC model is applied not only to the study of nuclear structure, but also to hadron physics, astrophysics, and particle physics [11–16].

The quark is treated as a current quark in QMC model, whose mass is very small, just several MeV. Accordingly, Toki *et al.* used a constituent quark model for the nucleon instead of the MIT bag model [17], named the quark mean field (QMF) model. The quarks are confined through some confinement potentials in the QMF model, whose constituent quark mass is around 300 MeV. Shen *et al.* promoted such a picture with more precise parameters by fitting the properties of stable finite nuclei [18] and applied it to the study of hypernuclei and neutron stars [19–21]. To include baryon octets, Wang *et al.* introduced a chiral Lagrangian at the hadron level in the QMF model and studied the properties of strangeness in nuclear matter [22–27].

In the QMC and QMF models, two very important factors in QCD theory are neglected. One is the gluon, which propagates the interaction of quarks. The other is chiral symmetry, which

^{*}hujinniu@nankai.edu.cn

is taken into account by pions and generates the quark mass from the chiral symmetry limit. The gluon can interact with itself and the contribution of the pion in the mean field is zero. Many works first attempted to consider the pion effect within the QMF model through the Fock term [28–30]. Recently, Nagai *et al.* extended the QMC model to include the gluon and pion exchange effect by using the cloudy bag model (CBM) [31]. Furthermore, Barik *et al.* calculated the contribution of the quark-pion interaction and the quark-gluon interaction by one-pion exchange and one-gluon exchange, respectively, in lowest-order perturbation theory in the 1980s [32,33].

Recently, Barik *et al.* developed their method from single baryon states to infinite nuclear matter following the methodology of the QMC and QMF models; they named it the MQMC model, and discussed the properties of symmetric nuclear matter influenced by the quark mass with σ and ω meson exchanges [34]. Later, they also included the ρ meson to study asymmetric nuclear mechanical instability and its dependence on the isospin asymmetry of the system [35]. In their works, the free parameters, such as the strengths of σ and ω mesons, are determined by the nuclear saturation properties. The nonlinear terms of σ and ω mesons were not included in the Lagrangian, which resulted in a large effective nucleon mass. Therefore, such parameter sets obtained by Barik *et al.* from nuclear matter could not describe the properties of finite nuclei very well.

Therefore, in this work, we would like to include the contribution of pions and gluons with perturbation theory in the QMF model and fix the free parameters from the ground states of stable finite nuclei. Then, we will apply such new parameters to study the properties of nuclear matter and neutron stars.

The paper is organized as follows. In Sec. II, we briefly derive the contribution of pions and gluons on nucleon properties with perturbation theory and the formulas of the QMF model for nuclear matter and finite nuclei. In Sec. III, new parameter sets of the QMF model with pion and gluon corrections will be determined. The properties of nuclear matter and finite nuclei with such new parameter sets will be shown. A summary is given in Sec. IV.

II. QUARK MEAN FIELD MODEL WITH PION AND GLUON CORRECTIONS

The analytical confinement potential for quarks cannot be obtained from QCD theory directly. Many phenomenological confinement potentials were proposed, where the polynomial forms were widely used. A harmonic oscillator potential, $U(r)$, is adopted in this work, with which the Dirac equation can be solved analytically [34]:

$$U(r) = \frac{1}{2}(1 + \gamma^0)(ar^2 + V_0), \quad (1)$$

where the scalar-vector form of the Dirac structure is chosen for the quark confinement potential. Here, we should emphasize that such a potential is just used for the baryon state, not for meson state, since in QMF model the degrees of freedom for quarks and mesons are equally treated. a and V_0 are the potential parameters, which are determined by the free nucleon mass and radius. When the effect of the nuclear medium is considered, the quark field $\psi_q(\vec{r})$ satisfies the following Dirac

equation:

$$\begin{aligned} & [\gamma^0(\epsilon_q - g_\omega^q \omega - \tau_{3q} g_\rho^q \rho) - \vec{\gamma} \cdot \vec{p} \\ & - (m_q - g_\sigma^q \sigma) - U(r)] \psi_q(\vec{r}) = 0, \end{aligned} \quad (2)$$

where σ , ω , and ρ are the classical meson fields, which take the exchanging interaction between quarks. g_σ^q , g_ω^q , and g_ρ^q are the coupling constants of σ , ω , and ρ mesons with quarks, respectively. τ_{3q} is the third component of the isospin matrix and m_q is the bare quark mass. Now we can define the following quantities for later convenience:

$$\begin{aligned} \epsilon'_q &= \epsilon_q^* - V_0/2, \\ m'_q &= m_q^* + V_0/2, \end{aligned} \quad (3)$$

where the effective single quark energy is given by $\epsilon_q^* = \epsilon_q - g_\omega^q \omega - \tau_{3q} g_\rho^q \rho$ and the effective quark mass by $m_q^* = m_q - g_\sigma^q \sigma$ [18]. We also introduce λ_q and r_{0q} as

$$\begin{aligned} \lambda_q &= \epsilon'_q + m'_q, \\ r_{0q} &= (a\lambda_q)^{-\frac{1}{4}}. \end{aligned} \quad (4)$$

The nucleon mass in the nuclear medium can be expressed as the binding energy of three quarks named the zeroth-order term, after solving the Dirac equation (2), formally

$$E_N^{*0} = \sum_q \epsilon_q^*. \quad (5)$$

The quarks are simply confined in a two-body confinement potential. Three corrections will be taken into account in the zeroth-order nucleon mass in the nuclear medium, including the center-of-mass correction $\epsilon_{c.m.}$, the pion correction δM_N^π , and the gluon correction $(\Delta E_N)_g$. The pion correction is generated by the chiral symmetry of QCD theory and the gluon correction by the short-range exchange interaction of quarks. The center-of-mass correction can be obtained [34] from

$$\epsilon_{c.m.} = \langle N | \mathcal{H}_{c.m.} | N \rangle, \quad (6)$$

where $\mathcal{H}_{c.m.}$ is the center-of-mass Hamiltonian density and $|N\rangle$ is the nucleon state. When the nucleon wave function is constructed by the quark wave functions, the center-of-mass correction comes out as

$$\epsilon_{c.m.} = \frac{77\epsilon'_q + 31m'_q}{3(3\epsilon'_q + m'_q)^2 r_{0q}^2}. \quad (7)$$

In order to restore the chiral symmetry in the nucleon, an elementary pion field is introduced in the present model. The pion contribution is zero in first-order perturbation theory due to its pseudovector properties. Therefore, we should treat it with second-order perturbation theory. Then, the pionic self-energy correction to the nucleon mass becomes

$$\delta M_B^\pi = - \sum_k \sum_{B'} \frac{V_j^{\dagger BB'} V_j^{BB'}}{w_k}, \quad (8)$$

where $\sum_k \equiv \sum_j \int d^3k / (2\pi)^3$, $w_k = (k^2 + m_\pi^2)^{1/2}$ is the pion energy, and $V_j^{BB'}$ represents the baryon pion absorption vertex function in the point-pion approximation. Then it can be

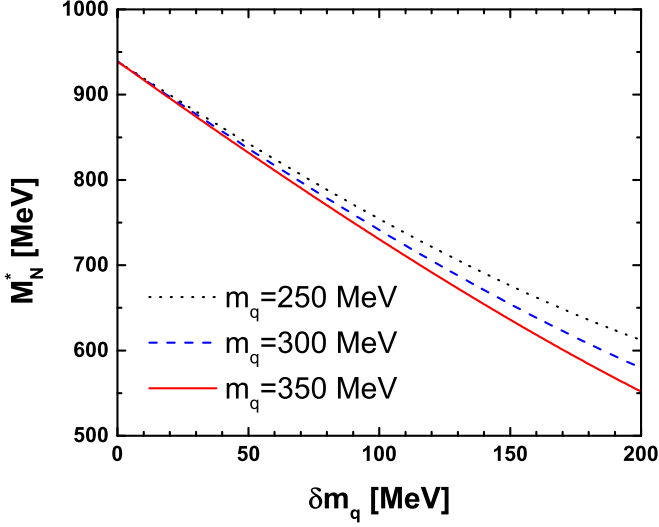


FIG. 1. The effective nucleon masses M_N^* as a function of the quark mass correction δm_q for quark masses $m_q = 250$ MeV (dotted curve), $m_q = 300$ MeV (dashed curve), and $m_q = 350$ MeV (solid curve).

simplified as

$$\delta M_N^\pi = -\frac{171}{25} I_\pi f_{NN\pi}^2, \quad (9)$$

where

$$I_\pi = \frac{1}{\pi m_\pi^2} \int_0^\infty dk \frac{k^4 u^2(k)}{w_k^2}, \quad (10)$$

with the axial-vector nucleon form factor

$$u(k) = \left[1 - \frac{3}{2} \frac{k^2}{\lambda_q (5\epsilon'_q + 7m'_q)} \right] e^{-\frac{1}{4} r_{0q}^2 k^2}, \quad (11)$$

and $f_{NN\pi}$ can be obtained from the Goldberg-Triemann relation by using the axial-vector coupling-constant value g_A in this model. The one-gluon exchange contribution to the mass is separated into two parts as

$$(\Delta E_B)_g = (\Delta E_B)_g^E + (\Delta E_B)_g^M, \quad (12)$$

where $(\Delta E_B)_g^E$ is the color-electric contribution

$$(\Delta E_B)_g^E = \frac{1}{8\pi} \sum_{i,j} \sum_{a=1}^8 \int \frac{d^3 r_i d^3 r_j}{|\vec{r}_i - \vec{r}_j|} \langle B | J_i^{0a}(\vec{r}_i) J_j^{0a}(\vec{r}_j) | B \rangle, \quad (13)$$

and $(\Delta E_B)_g^M$ the color-magnetic contribution

$$(\Delta E_B)_g^M = -\frac{1}{8\pi} \sum_{i,j} \sum_{a=1}^8 \int \frac{d^3 r_i d^3 r_j}{|\vec{r}_i - \vec{r}_j|} \langle B | \vec{J}_i^a(\vec{r}_i) \cdot \vec{J}_j^a(\vec{r}_j) | B \rangle. \quad (14)$$

Here

$$J_i^{\mu a}(x) = g_c \bar{\psi}_q(x) \gamma^\mu \lambda_i^a \psi_q(x) \quad (15)$$

is the quark color current density, where λ_i^a are the usual Gell-Mann SU(3) matrices and $\alpha_c = g_c^2/4\pi$. Then Eqs. (13) and (14) can be written as

$$(\Delta E_N)_g^E = \alpha_c (b_{uu} I_{uu}^E + b_{us} I_{us}^E + b_{ss} I_{ss}^E), \quad (16)$$

and

$$(\Delta E_N)_g^M = \alpha_c (a_{uu} I_{uu}^M + a_{us} I_{us}^M + a_{ss} I_{ss}^M), \quad (17)$$

where a_{ij} and b_{ij} are the numerical coefficients depending on each baryon and the quantities I_{ij}^E and I_{ij}^M are given in the following equations:

$$I_{ij}^E = \frac{16}{3\sqrt{\pi}} \frac{1}{R_{ij}} \left[1 - \frac{\alpha_i + \alpha_j}{R_{ij}^2} + \frac{3\alpha_i \alpha_j}{R_{ij}^4} \right], \quad (18)$$

$$I_{ij}^M = \frac{256}{9\sqrt{\pi}} \frac{1}{R_{ij}^3} \frac{1}{(3\epsilon'_i + m'_i)} \frac{1}{(3\epsilon'_j + m'_j)},$$

with

$$R_{ij}^2 = 3 \left[\frac{1}{(\epsilon'_i{}^2 - m'_i{}^2)} + \frac{1}{(\epsilon'_j{}^2 - m'_j{}^2)} \right], \quad (19)$$

$$\alpha_i = \frac{1}{(\epsilon'_i + m'_i)(3\epsilon'_i + m'_i)}.$$

Finally, taking the above pion and gluon corrections, the mass of the nucleon in the nuclear medium becomes

$$M_N^* = E_N^{*0} - \epsilon_{c.m.} + \delta M_N^\pi + (\Delta E_N)_g^E + (\Delta E_N)_g^M. \quad (20)$$

Until now, we have constructed the nucleon at quark level with confinement potential and the pion and gluon corrections. Next, we would like to connect such a nucleon in the nuclear medium with nuclear objects, such as nuclear matter and a finite nuclei system. A good bridge is the relativistic mean field (RMF) model at hadron level, which was developed based on the one-boson exchange potential between two nucleons.

TABLE I. The parameters for quarks and hadrons are listed. The first parameter set corresponding to $m_q = 250$ MeV is named QMF-NK1, the second for $m_q = 300$ MeV is named QMF-NK2, and the third for $m_q = 350$ MeV is named QMF-NK3.

m_q (MeV)	g_σ^q	g_ω	g_ρ	g_2 (fm ⁻¹)	g_3	c_3	a (fm ⁻³)	V_0 (MeV)
250	5.15871	11.54726	3.79601	-3.52737	-78.52006	305.00240	0.57945	-24.28660
300	5.09346	12.30084	4.04190	-3.42813	-57.68387	249.05654	0.53430	-62.25719
350	5.01631	12.83898	4.10772	-3.29969	-39.87981	221.68240	0.49560	-102.04158

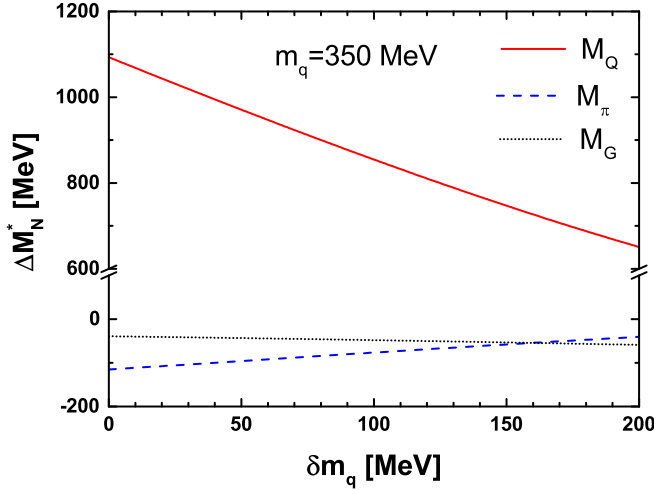


FIG. 2. The contributions of confinement potential, pion correction, and gluon correction to the effective nucleon mass M_N^* as a function of the quark mass correction δm_q at quark mass $m_q = 350$ MeV. M_Q , M_π , and M_G represent the confinement contribution, pion correction, and gluon correction, respectively.

The effective nucleon mass from the quark model will be inserted to the RMF Lagrangian. The nucleon and meson fields will be solved self-consistently, and then the properties of the nuclear many-body system will be obtained. We would like to use a more complicated Lagrangian and compare with the MQMC model [34]. The MQMC parameter sets without nonlinear terms of σ and ω mesons can provide very good saturation properties of nuclear matter, but for the description of finite nuclei they cannot give results of binding energies and charge radii consistent with the experimental data. For example, with $m_q = 300$ MeV in the MQMC model, the total energy difference of ^{208}Pb between theoretical calculation and experimental data is about 80 MeV. Meanwhile, in the MQMC model, the effective nucleon mass at saturation density is a little bit larger than the empirical data, which will generate a small spin-orbit splitting comparing with the experimental observation. Therefore, we should introduce the nonlinear terms of σ and ω mesons at the nucleon level. At the same time, in this work, we just consider the σ , ω , and ρ meson exchange in the QMF Lagrangian [18], which is

given as

$$\begin{aligned} \mathcal{L}_{\text{QMF}} = & \bar{\psi} \left[i\gamma_\mu \partial^\mu - M_N^* - g_\omega \omega \gamma^0 - g_\rho \rho \tau_3 \gamma^0 \right. \\ & \left. - e \frac{(1 - \tau_3)}{2} A \gamma^0 \right] \psi \\ & - \frac{1}{2} (\nabla \sigma)^2 - \frac{1}{2} m_\sigma^2 \sigma^2 - \frac{1}{3} g_2 \sigma^3 - \frac{1}{4} g_3 \sigma^4 \\ & + \frac{1}{2} (\nabla \omega)^2 + \frac{1}{2} m_\omega^2 \omega^2 + \frac{1}{4} c_3 \omega^4 \\ & + \frac{1}{2} (\nabla \rho)^2 + \frac{1}{2} m_\rho^2 \rho^2 + \frac{1}{2} (\nabla A)^2, \end{aligned} \quad (21)$$

where M_N^* is the effective nucleon mass obtained from the quark model, and the coupling constants of ω and ρ mesons with the nucleon can be related to the quark part as $g_\omega = 3g_\omega^q$ and $g_\rho = g_\rho^q$ according to the quark counting rules. A is the electromagnetic field for the Coulomb interaction between protons. In this Lagrangian, we already consider the static approximation for the mesons so that their time components are neglected. The spatial part of the ω meson disappears for time reversal symmetry.

From this Lagrangian, the equations of motion of nucleons and mesons will be generated by the Euler-Lagrangian equation,

$$\begin{aligned} & \left[i\gamma_\mu \partial^\mu - M_N^* - g_\omega \omega(r) \gamma^0 - g_\rho \rho(r) \tau_3 \gamma^0 \right. \\ & \left. - e \frac{(1 - \tau_3)}{2} A(r) \gamma^0 \right] \psi = 0, \\ \Delta \sigma(r) - m_\sigma^2 \sigma(r) - g_2 \sigma^2(r) - g_3 \sigma^3(r) &= \frac{\partial M_N^*}{\partial \sigma} \langle \bar{\psi} \psi \rangle, \\ \Delta \omega(r) - m_\omega^2 \omega(r) - c_3 \omega^3(r) &= -g_\omega \langle \bar{\psi} \gamma^0 \psi \rangle, \\ \Delta \rho(r) - m_\rho^2 \rho(r) &= -g_\rho \langle \bar{\psi} \tau_3 \gamma^0 \psi \rangle, \\ \Delta A(r) &= -e \langle \bar{\psi} \frac{(1 - \tau_3)}{2} \gamma^0 \psi \rangle, \end{aligned} \quad (22)$$

where $\frac{\partial M_N^*}{\partial \sigma}$ comes from the quark model and is different from the g_σ in RMF model. Here we restrict our consideration to spherically symmetric nuclei and r is the radial coordinate of the nuclear center. These equations of motion can be solved self-consistently in a numerical program. From the

TABLE II. The binding energies per nucleon E/A and the rms charge radii R_c with QMF-NK1, QMF-NK2, and QMF-NK3 parameter sets, compared with the results in the previous QMF model without pion and gluon corrections, and experimental values.

Model	E/A (MeV)				R_c (fm)			
	^{40}Ca	^{48}Ca	^{90}Zr	^{208}Pb	^{40}Ca	^{48}Ca	^{90}Zr	^{208}Pb
QMF-NK1	8.62	8.61	8.65	7.92	3.43	3.47	4.26	5.49
QMF-NK2	8.61	8.61	8.67	7.91	3.44	3.47	4.26	5.50
QMF-NK3	8.59	8.63	8.68	7.90	3.44	3.46	4.26	5.50
QMF [18]	8.35	8.43	8.54	7.73	3.44	3.46	4.27	5.53
Expt.	8.55	8.67	8.71	7.87	3.45	3.45	4.26	5.50

TABLE III. The spin-orbit splittings of ^{40}Ca and ^{208}Pb for QMF-NK1, QMF-NK2, and QMF-NK3, compared with the experimental data. All quantities are in MeV.

Model	^{40}Ca		^{208}Pb	
	Proton ($1d_{5/2}-1d_{3/2}$)	Neutron ($1d_{5/2}-1d_{3/2}$)	Proton ($1g_{9/2}-1g_{7/2}$)	Neutron ($2f_{7/2}-2f_{5/2}$)
QMF-NK1	-3.7	-3.7	-2.4	-1.5
QMF-NK2	-4.5	-4.5	-2.8	-1.7
QMF-NK3	-5.1	-5.1	-3.2	-1.9
Expt.	-7.2	-6.3	-4.0	-1.8

single-particle energies of the nucleons, the total energy of whole nucleus can be obtained with the mean field method.

Infinite nuclear matter, which does not really exist in universe, is very helpful for us to understand the basic physics of the nuclear many-body system. It has the translational invariance in an infinite system, which removes the partial part on coordinate space. Its Lagrangian density and equations of motion will be written as

$$\begin{aligned} \mathcal{L}_{\text{QMF}} = & \bar{\psi}(i\gamma_{\mu}\partial^{\mu} - M_N^* - g_{\omega}\omega\gamma^0 - g_{\rho}\rho\tau_3\gamma^0)\psi \\ & - \frac{1}{2}m_{\sigma}^2\sigma^2 - \frac{1}{3}g_2\sigma^3 - \frac{1}{4}g_3\sigma^4 \\ & + \frac{1}{2}m_{\omega}^2\omega^2 + \frac{1}{4}c_3\omega^4 + \frac{1}{2}m_{\rho}^2\rho^2, \end{aligned} \quad (23)$$

and

$$\begin{aligned} (i\gamma^{\mu}\partial_{\mu} - M_N^* - g_{\omega}\omega\gamma^0 - g_{\rho}\rho\tau_3\gamma^0)\psi &= 0, \\ m_{\sigma}^2\sigma + g_2\sigma^2 + g_3\sigma^3 &= -\frac{\partial M_N^*}{\partial\sigma}\langle\bar{\psi}\psi\rangle, \\ m_{\omega}^2\omega + c_3\omega^3 &= g_{\omega}\langle\bar{\psi}\gamma^0\psi\rangle, \\ m_{\rho}^2\rho &= g_{\rho}\langle\bar{\psi}\tau_3\gamma^0\psi\rangle. \end{aligned} \quad (24)$$

From this Lagrangian and these equations of motion of nucleon and mesons, the energy density and pressure can be generated

by the energy-momentum tensor [36],

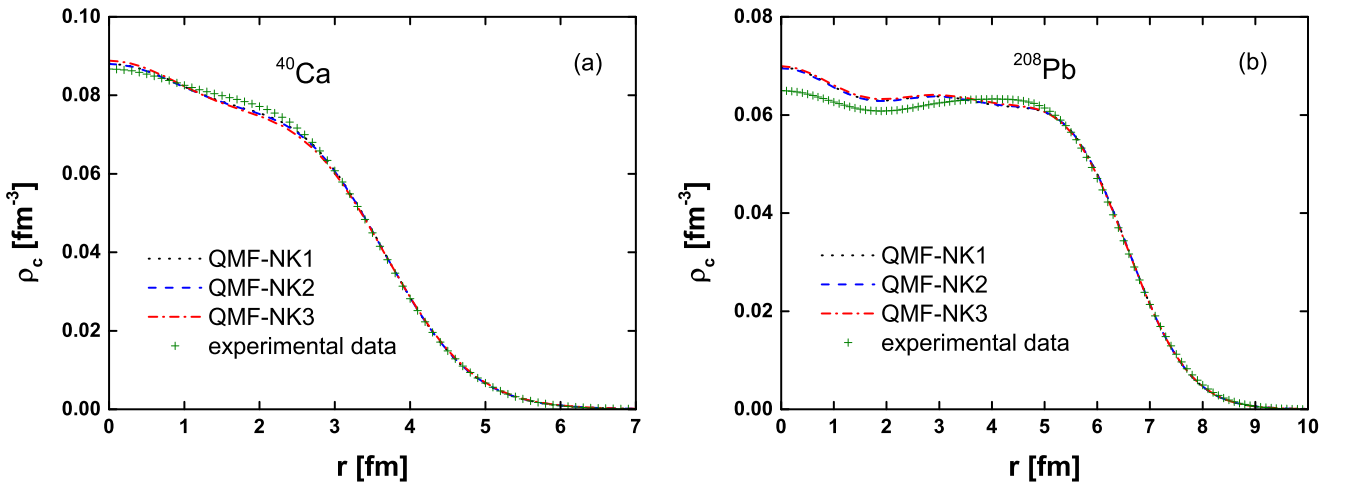
$$\begin{aligned} \mathcal{E}_{\text{QMF}} = & \sum_{i=n,p} \frac{1}{\pi^2} \int_0^{k_f} \sqrt{k^2 + M^*k^2} dk \\ & + \frac{1}{2}m_{\sigma}^2\sigma^2 - \frac{1}{3}g_2\sigma^3 + \frac{1}{4}g_3\sigma^4 \\ & + \frac{1}{2}m_{\omega}^2\omega^2 + \frac{3}{4}c_3\omega^4 + \frac{1}{2}m_{\rho}^2\rho^2 \end{aligned} \quad (25)$$

and

$$\begin{aligned} P_{\text{QMF}} = & \frac{1}{3\pi^2} \sum_{i=n,p} \int_0^{k_f} \frac{k^4}{\sqrt{k^2 + M^*}} dk \\ & - \frac{1}{2}m_{\sigma}^2\sigma^2 + \frac{1}{3}g_2\sigma^3 - \frac{1}{4}g_3\sigma^4 \\ & + \frac{1}{2}m_{\omega}^2\omega^2 + \frac{1}{4}c_3\omega^4 + \frac{1}{2}m_{\rho}^2\rho^2. \end{aligned} \quad (26)$$

III. RESULTS AND DISCUSSIONS

The parameters of the confinement potential (a, V_0) are determined by the experimental data of nucleon mass $M_N = 939$ MeV and charge radius $\langle r_N^2 \rangle^{1/2} = 0.87$ fm in free space. Then we calculate the effective mass M_N^* in the nuclear medium as a function of the quark mass correction δm_q , which is defined as $\delta m_q = m_q - m_q^* = g_{\sigma}^q$.


 FIG. 3. The charge density distributions of ^{40}Ca (a) and ^{208}Pb (b) for QMF-NK1, QMF-NK2, and QMF-NK3 compared with the experimental data.

In Fig. 1, the effective nucleon masses with different bare quark masses ($m_q = 250, 300,$ and 350 MeV) are given as functions of quark mass correction. The values of (a, V_0) in different quark masses are given in Table I. In free space ($\delta m_q = 0$), their effective masses completely correspond to the free nucleon mass. With δm_q increasing, the effective nucleon masses will be reduced from the effect of surrounding nucleons. Furthermore, this reduction becomes more pronounced at larger quark mass.

We also show the contributions from the quark confinement, pion correction, and gluon correction on the effective nucleon mass in Fig. 2. The confinement potential provides a positive contribution to the effective nucleon mass and largely reduces the effective mass in the nuclear medium, while the pion and gluon generate the negative contribution to the nucleon mass. The gluon correction is almost not influenced by the nuclear medium, and the pion one increases slowly with δm_q . Their magnitudes are smaller compared to the one from the confinement potential, and are calculated with the perturbation theory.

After we fix the parameters of the quark confinement potential, the coupling constants between quarks and mesons should be determined by the properties of finite nuclei. In this work, we take the meson masses as $m_\sigma = 550$ MeV, $m_\omega = 783$ MeV, and $m_\rho = 763$ MeV. $g_\sigma^q, g_\omega, g_\rho, g_2, g_3,$ and c_3 will be fitted by the binding energies per nucleon E/A and the charge radii R_c of four closed shell nuclei, $^{40}\text{Ca}, ^{48}\text{Ca}, ^{90}\text{Zr},$ and ^{208}Pb , with a least-squares fitting method. Three parameter sets are achieved at $m_q = 250, 300,$ and 350 MeV to study the effect of quark properties on the nuclear many-body system. These parameters sets and the corresponding a and V_0 in the quark confinement potential are listed in Table I. For convenience in later discussion, we name the first parameter set ($m_q = 250$ MeV) in Table I as QMF-NK1, the second ($m_q = 300$ MeV) as QMF-NK2, and the third ($m_q = 350$ MeV) as QMF-NK3.

In Table II, the results of theoretical calculation for the binding energies per nucleon E/A and the charge radii R_c for four spherically symmetric nuclei, $^{40}\text{Ca}, ^{48}\text{Ca}, ^{90}\text{Zr},$ and ^{208}Pb , by QMF-NK1, QMF-NK2, and QMF-NK3 are compared with the experimental data. We can find that the results from the QMF-NK3 are closest to the experimental values compared to the other two parameter sets. It demonstrates that the heavier quark mass is more acceptable for the nuclear many-body system. The calculation without the pion and gluon corrections by Shen and Toki [18] is also compared and the present results are largely improved. Therefore, it is necessary to include the contributions of pions and gluons to describe the finite nuclei system properly.

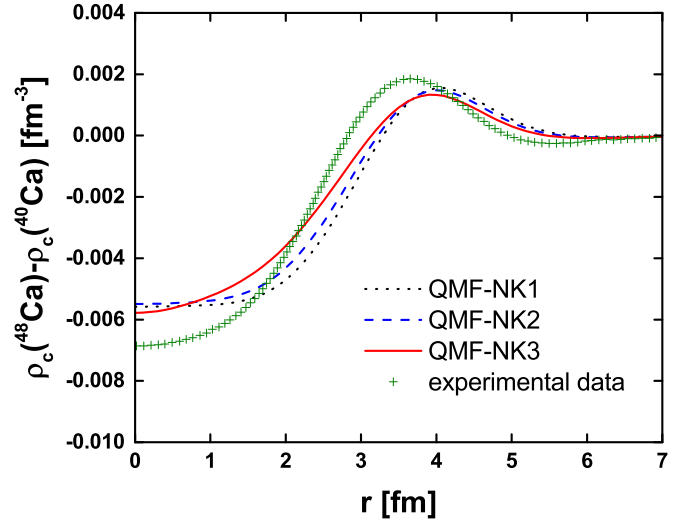


FIG. 4. The difference between the ^{48}Ca and ^{40}Ca charge densities for QMF-NK1, QMF-NK2, and QMF-NK3, compared with the experimental data.

In Table III, we also compare the spin-orbit splittings of ^{40}Ca and ^{208}Pb for QMF-NK1, QMF-NK2, and QMF-NK3 in the present work to the experimental data. With increasing quark mass, the spin-orbit splittings of these nuclei become larger and approach the experimental data. In the RMF model, the spin-orbit splittings are actually strongly dependent on the effective nucleon mass and have the inverse relation. From Fig. 1, we can observe that the largest quark mass generates the smallest effective nucleon mass at each δm_q . Therefore, a large quark mass will result in a large spin-orbit splitting.

In Fig. 3, we plot the charge density distributions of ^{40}Ca and ^{208}Pb for QMF-NK1, QMF-NK2, and QMF-NK3 and compare them with the experimental data. They are almost identical for the three parameter sets and coincident with the behavior of experimental data. In Fig. 4, we also plot the difference between the ^{48}Ca and ^{40}Ca charge densities for QMF-NK1, QMF-NK2, and QMF-NK3.

Once we have fixed the free parameters in the QMF Lagrangian from the finite nuclei system, we can apply such parameter sets to the study of nuclear matter and examine their validity. In Table IV, the various properties of symmetric nuclear matter at saturation density for the three parameter sets are tabulated, such as saturation density, binding energy per particle, incompressibility, symmetry energy, and so on. Their detailed expressions can be found in Ref. [35]. The saturation densities, binding energies, and incompressibilities for QMF-NK1, QMF-NK2, and QMF-NK3 are almost the same, which

TABLE IV. Saturation properties of nuclear matter in the QMF-NK1, QMF-NK2, and QMF-NK3 parameter sets.

Model	ρ_0 (fm^{-3})	E/A (MeV)	K_0 (MeV)	J (MeV)	M_N^*/M_N	L^0 (MeV)	K_{sym}^0 (MeV)	K_{asy} (MeV)	Q_0 (MeV)	K_τ (MeV)
QMF-NK1	0.154	-16.3	323	30.6	0.70	84.8	-28.8	-537.6	495.4	-667.7
QMF-NK2	0.152	-16.3	328	32.9	0.66	93.7	-23.5	-585.7	221.0	-648.8
QMF-NK3	0.150	-16.3	322	33.6	0.64	97.3	-12.0	-595.8	263.0	-675.3

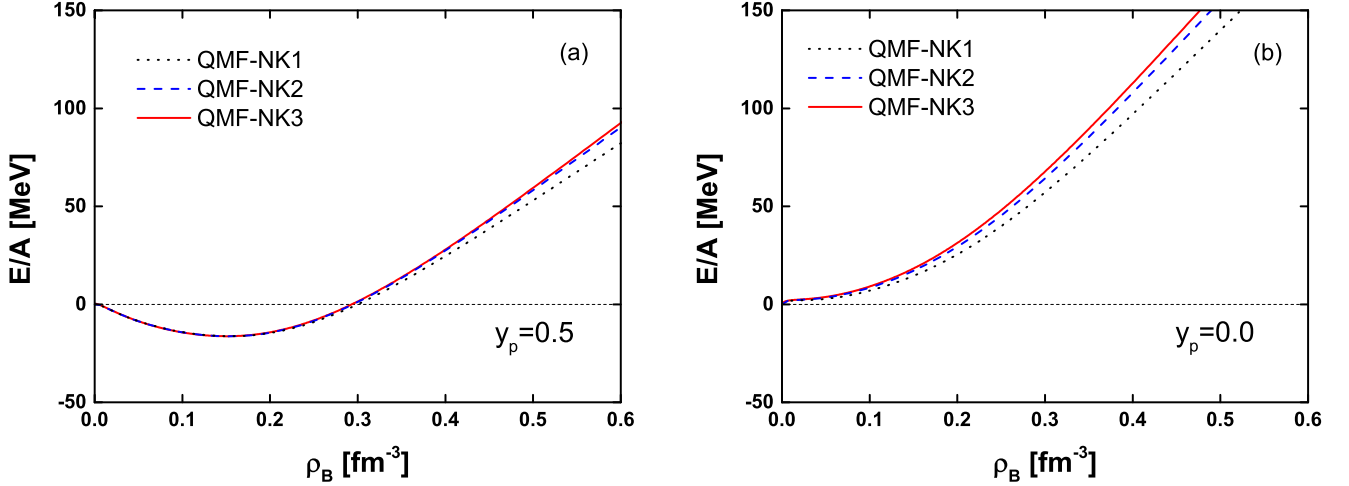


FIG. 5. EOSs of symmetric nuclear matter and pure neutron matter in QMF-NK1, QMF-NK2, and QMF-NK3 for (a) $y_p = 0.5$ and (b) $y_p = 0.0$.

is consistent with the empirical saturation properties of nuclear matter. The symmetry energies and effective masses obviously perform differently for these three parameter sets, which is caused by the coupling constants of the ρ meson and quark masses.

In Fig. 5, we plot nuclear matter binding energy as a function of density for the three parameter sets for symmetric nuclear matter and pure neutron matter. At low densities, the equations of state (EOS) for different sets are identical. With increasing density, the EOS becomes softer for lower quark mass.

The neutron star as a natural laboratory is a very good object to check the nuclear theoretical model. We calculate the properties of neutron stars with the QMF model and show the mass-radius relations for neutron stars in Fig. 6. The maximum masses of neutron star in this work are between $2.25M_\odot$ and $2.38M_\odot$, which satisfies the constraint of present astronomical observation data, about $2M_\odot$ [37]. However, the previous QMF

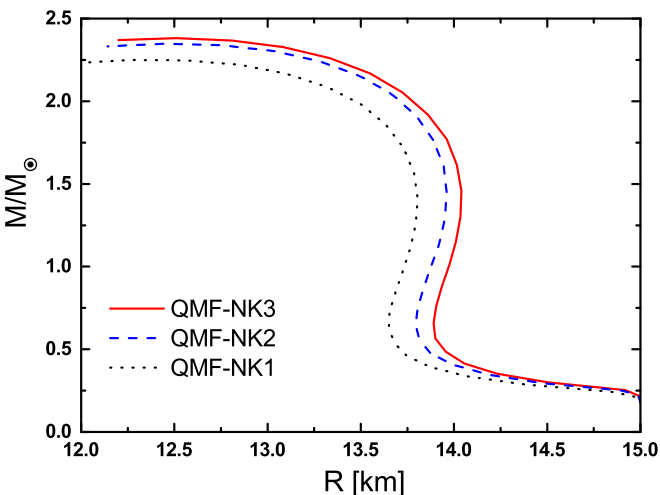


FIG. 6. The mass-radius relations for neutron stars with QMF-NK1, QMF-NK2, and QMF-NK3.

model without pion and gluon corrections could not provide a large neutron star mass [21].

IV. CONCLUSION

We studied the properties of finite nuclei and infinite nuclear matter in terms of the quark mean field (QMF) model with the effects of pions and gluons. In the QMF model, the nucleon is made up of three constituent quarks with a confinement potential. Due to the chiral symmetry in QCD theory and the quark exchange interaction, the corrections of pions and gluons have been considered in a perturbation manner to obtain the effective nucleon mass in the medium. The strength of confinement potential is determined by the mass and charge radius of the free nucleon. For the hadron part of the QMF model, the nucleon is combined through the meson exchange between quarks. Compared to the previous MQMC model [34], we also included the nonlinear terms of σ and ω mesons. Their coupling constants (g_σ^q , g_ω , g_ρ , g_2 , g_3 , and c_3) were determined by fitting the experimental data of the binding energies per nucleon E/A and the charge radii R_c of four closed-shell nuclei, ^{40}Ca , ^{48}Ca , ^{90}Zr , and ^{208}Pb . Finally, we obtained three parameter sets with different quark confinement potentials, named QMF-NK1, QMF-NK2, and QMF-NK3. The present QMF model is largely improved to describe the properties of finite nuclei compared to the previous QMF version without pion and gluon corrections and to the MQMC model. The MQMC parameter sets without nonlinear terms of σ and ω mesons could provide very good saturation properties of nuclear matter, but for the description of finite nuclei they cannot give results of binding energies and charge radii consistent with the experimental data. For example, with $m_q = 300$ MeV in the MQMC model, the total energy difference of ^{208}Pb between theoretical calculation and experimental data is about 80 MeV. After we introduced the nonlinear terms of σ and ω mesons, this difference was reduced to 6 MeV with the QMF-NK3 parameter set, while the saturation properties of nuclear matter were still kept in very good agreement. Furthermore, we also calculated

the spin-orbit splittings for ^{40}Ca and ^{208}Pb , and the charge density distributions in comparison with the experimental data. The spin-orbit splittings in our work were largely improved compared to the ones in the MQMC model, where the effective nucleon mass was very large at saturation density to generate small spin-orbit splittings of finite nuclei. We also found that the spin-orbit splittings increased with the quark mass, since a smaller effective nucleon mass usually generates strong spin-orbit force in the RMF framework.

We also applied these parameter sets to the study of infinite nuclear matter. The various saturation properties of symmetric nuclear matter are consistent with the empirical data. The obvious difference in QMF-NK1, QMF-NK2, and QMF-NK3 are reflected in the symmetry energies and effective nucleon masses at saturation density, which were strongly dependent on the strength of ρ meson coupling with quarks and the quark mass. The equations of state (EOSs) of symmetry nuclear matter and pure neutron matter were given, where the EOS with large quark mass became stiffer. The mass-radius relations of neutron stars were calculated. The maximum neutron star masses in the present QMF model were around $2.25M_{\odot}$ to $2.38M_{\odot}$, which satisfied the recent constraint of astrophysics

observation. Recently, there have been many discussions on the hyperon degrees of freedom for massive neutron stars, which is called the “hyperon puzzle.” In the future, we will include the strange quark degree of freedom in the quark level to generate more baryon states, such as Λ , Σ , and Ξ to study the hyperon degrees of freedom in neutron stars.

With the pion and gluon corrections, the QMF model could treat finite nuclei and nuclear matter better. Although it is a long road to describe the nuclear many-body system with QCD theory directly, the influence of quark level on nuclear structure was found in the present QMF model, e.g., in the effective nucleon mass. With the energy and density increasing, the strangeness degree of freedom will appear in nuclear physics. We will consider more baryon states in such models and study their roles in hypernuclei and neutron stars.

ACKNOWLEDGMENTS

We are grateful for detailed and fruitful discussions with Prof. Hiroshi Toki and Dr. Ang Li. This work was supported in part by the National Natural Science Foundation of China (Grants No. 11375089 and No. 11405090).

-
- [1] K. Jansen, Proc. Sci. **LATTICE2008**, 010 (2008), [arXiv:0810.5634](#).
- [2] S. C. Pieper and R. B. Wiringa, *Annu. Rev. Nucl. Part. Sci.* **51**, 53 (2001).
- [3] E. Caurier, G. Martínez-Pinedo, F. Nowacki, A. Poves, and A. P. Zuker, *Rev. Mod. Phys.* **77**, 427 (2005).
- [4] J. Erler, P. Kluepel, and P.-G. Reinhard, *J. Phys. G* **38**, 033101 (2011).
- [5] B. D. Serot and J. D. Walecka, *Adv. Nucl. Phys.* **16**, 1 (1986).
- [6] P. A. M. Guichon, *Phys. Lett. B* **200**, 235 (1988).
- [7] K. Saito and A. W. Thomas, *Phys. Lett. B* **327**, 9 (1994); **335**, 17 (1994); **363**, 157 (1995).
- [8] P. A. M. Guichon, K. Saito, E. Rodionov, and A. W. Thomas, *Nucl. Phys. A* **601**, 349 (1996).
- [9] K. Saito, K. Tsushima, and A. W. Thomas, *Nucl. Phys. A* **609**, 339 (1996); *Phys. Rev. C* **55**, 2637 (1997); *Phys. Lett. B* **406**, 287 (1997).
- [10] J. J. Aubert *et al.* (EMC Collaboration), *Phys. Lett. B* **123**, 275 (1983).
- [11] P. K. Panda, A. Mishra, J. M. Eisenberg, and W. Greiner, *Phys. Rev. C* **56**, 3134 (1997).
- [12] P. K. Panda, R. Sahu, and C. Das, *Phys. Rev. C* **60**, 038801 (1999).
- [13] P. K. Panda, G. Krein, D. P. Menezes, and C. Providencia, *Phys. Rev. C* **68**, 015201 (2003).
- [14] P. K. Panda, D. P. Menezes, and C. Providencia, *Phys. Rev. C* **69**, 025207 (2004).
- [15] P. K. Panda, A. M. S. Santos, D. P. Menezes, and C. Providencia, *Phys. Rev. C* **85**, 055802 (2012).
- [16] K. Saito, K. Tsushima, and A. W. Thomas, *Prog. Part. Nucl. Phys.* **58**, 1 (2007).
- [17] H. Toki, U. Meyer, A. Faessler, and R. Brockmann, *Phys. Rev. C* **58**, 3749 (1998).
- [18] H. Shen and H. Toki, *Phys. Rev. C* **61**, 045205 (2000).
- [19] H. Shen and H. Toki, *Nucl. Phys. A* **707**, 469 (2002).
- [20] J. N. Hu, A. Li, H. Shen, and H. Toki, *Prog. Theor. Exp. Phys.* **2014**, 013D02 (2014).
- [21] J. N. Hu, A. Li, H. Toki, and W. Zuo, *Phys. Rev. C* **89**, 025802 (2014).
- [22] P. Wang, Z. Y. Zhang, Y. W. Yu, R. K. Su, and H. Q. Song, *Nucl. Phys. A* **688**, 791 (2001).
- [23] P. Wang, H. Guo, Z. Y. Zhang, Y. W. Yu, R. K. Su, and H. Q. Song, *Nucl. Phys. A* **705**, 455 (2002).
- [24] P. Wang, V. E. Lyubovitskij, T. Gutsche, and A. Faessler, *Phys. Rev. C* **67**, 015210 (2003).
- [25] P. Wang, D. B. Leinweber, A. W. Thomas, and A. G. Williams, *Nucl. Phys. A* **744**, 273 (2004).
- [26] P. Wang, D. B. Leinweber, A. W. Thomas, and A. G. Williams, *Phys. Rev. C* **70**, 055204 (2004).
- [27] P. Wang, D. B. Leinweber, A. W. Thomas, and A. G. Williams, *Nucl. Phys. A* **748**, 226 (2005).
- [28] G. Krein, A. W. Thomas, and K. Tsushima, *Nucl. Phys. A* **650**, 313 (1999).
- [29] J. R. Stone, P. A. M. Guichon, H. H. Matevosyan, and A. W. Thomas, *Nucl. Phys. A* **792**, 341 (2007).
- [30] D. L. Whittenbury, J. D. Carroll, A. W. Thomas, K. Tsushima, and J. R. Stone, *Phys. Rev. C* **89**, 065801 (2014).
- [31] S. Nagai, T. Miyatsu, K. Saito, and K. Tsushima, *Phys. Lett. B* **666**, 239 (2008).
- [32] N. Barik, B. K. Dash, and M. Das, *Phys. Rev. D* **31**, 1652 (1985); **32**, 1725 (1985).
- [33] N. Barik and B. K. Dash, *Phys. Rev. D* **33**, 1925 (1986); **34**, 2092 (1986).
- [34] N. Barik, R. N. Mishra, D. K. Mohanty, P. K. Panda, and T. Frederico, *Phys. Rev. C* **88**, 015206 (2013).
- [35] R. N. Mishra, H. S. Sahoo, P. K. Panda, N. Barik, and T. Frederico, *Phys. Rev. C* **92**, 045203 (2015).
- [36] H. Shen, *Phys. Rev. C* **65**, 035802 (2002).
- [37] P. B. Demorest, T. Pennucci, S. M. Ransom, M. S. E. Roberts, and J. W. T. Hessels, *Nature (London)* **467**, 1081 (2010); J. Antoniadis, P. C. C. Freire, N. Wex, T. M. Tauris, R. S. Lynch *et al.*, *Science* **340**, 6131 (2013).